Kinetic Relationship between the Voltage Sensor and the Activation Gate in spHCN Channels

Andrew Bruening-Wright,[1] Fredrik Elinder,[2] and H. Peter Larsson[1]

[1]Neurological Sciences Institute, Oregon Health and Science University, Beaverton, OR 97006
[2]Department of Biomedicine and Surgery, Division of Cell Biology, Linköpings Universitet, SE-581 85 Linköping, Sweden

Hyperpolarization-activated cyclic nucleotide-gated (HCN) channels are activated by membrane hyperpolarizations that cause an inward movement of the positive charges in the fourth transmembrane domain (S4), which triggers channel opening. The mechanism of how the motion of S4 charges triggers channel opening is unknown. Here, we used voltage clamp fluorometry (VCF) to detect S4 conformational changes and to correlate these to the different activation steps in spHCN channels. We show that S4 undergoes two distinct conformational changes during voltage activation. Analysis of the fluorescence signals suggests that the N-terminal region of S4 undergoes conformational changes during a previously characterized mode shift in HCN channel voltage dependence, while a more C-terminal region undergoes an additional conformational change during gating charge movements. We fit our fluorescence and ionic current data to a previously proposed 10-state allosteric model for HCN channels. Our results are not compatible with a fast S4 motion and rate-limiting channel opening. Instead, our data and modeling suggest that spHCN channels open after only two S4s have moved and that S4 motion is rate limiting during voltage activation of spHCN channels.

The Journal of General Physiology

INTRODUCTION

In pacemaking cells (Brown and DiFrancesco, 1980; Maylie et al., 1981; Maylie and Morad, 1984), hyperpolarization-activated cyclic nucleotide-gated (HCN) channels activate during the hyperpolarizing phase of the pacemaker cycle and depolarize excitable cells toward the threshold for the firing of the next action potential. HCN channels are also expressed in a broad range of cells and have been suggested to play an important role in dendritic integration, in synaptic transmission, in determining the resting-membrane properties, and in reducing extreme hyperpolarizations (DiFrancesco, 1993; Pape, 1996). Deletion of HCN channels by knockout techniques has resulted in mice with motor deficiencies, epilepsy, altered spatial learning, heart arrhythmia, and/or nonfunctional hearts, suggesting that HCN channels have widespread importance in the nervous system (Ludwig et al., 2003; Nolan et al., 2003; Schulze-Bahr et al., 2003; Ueda et al., 2004).

HCN channels belong to the super family of voltage-gated ion channels (Gauss et al., 1998). Most of the channels in this family, such as voltage-gated potassium, sodium, and calcium channels, are activated by an outward movement of positive charges in the S4 domain in response to membrane depolarization (Hille, 2001). However, HCN channels open by inward movement of the positive charges in S4 in response to membrane hyperpolarization (Mannikko et al., 2002; Sesti et al., 2003; Bell et al., 2004; Vemana et al., 2004). It is not known why HCN channels open by an inward S4 movement while other members of this family open by an outward S4 movement, but it has been suggested that the coupling of S4 to the channel gate is different in HCN channels than in the depolarization-activated ion channels (Mannikko et al., 2002). How S4 movement couples to the opening and closing of the activation gate in HCN channels is not known.

In contrast to classic "Hodgkin-Huxley"–type K channels that open with very sigmoidal activation kinetics (well described by the 4th power of an exponential rise time), tetrameric HCN channels open with a sigmoidicity around 2 (a range of 1–3 has been reported) (DiFrancesco, 1984, 1999; Altomare et al., 2001). In addition, the closing of HCN channels has a high sigmoidicity (power of 4) (Mannikko et al., 2005), in contrast to the exponentially decaying tail currents in most other voltage-activated channels. A model for HCN channel activation that can explain the low sigmoidicity has been proposed (Altomare et al., 2001). In this type of model, the four independent S4s rapidly move, followed by a slow opening of the activation gate (Fig. 1). This type of model does not generate a high sigmoidicity, since the movement of the four different S4s is faster than channel opening. Because the rate of activation of HCN channels is strongly voltage dependent, the authors had to propose a strong voltage dependence in the rate-limiting

Correspondence to H. Peter Larsson: larssonp@ohsu.edu

Abbreviations used in this paper: HCN, hyperpolarization-activated cyclic nucleotide-gated; S4, fourth transmembrane domain; VCF, voltage clamp fluorometry.

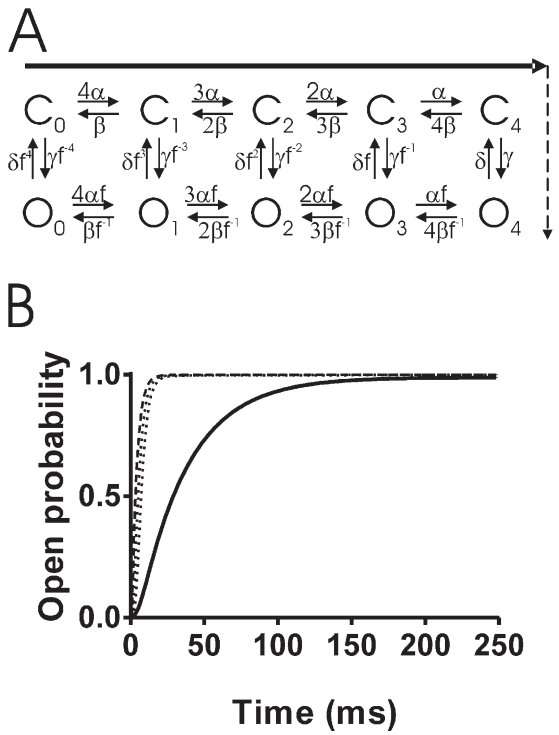

Figure 1. Predicted kinetic relationship between S4 movement and ionic currents at −120 mV for a published HCN channel model (Altomare et al., 2001). (A) State diagram for the Altomare model. There are four independent fast S4 movements (horizontal transitions) and slow rate-limiting activation-gate (vertical) transition. Both the S4 movement and the gate opening transitions are highly voltage dependent. The arrow on the state diagram denotes the most likely transition pathway. The continuous arrow denotes fast transitions and the dashed line slow transitions. At −120 mV, $\alpha = 289.7\ s^{-1}$, $\beta = 0.59\ s^{-1}$, $\gamma = 30.2\ s^{-1}$, $\delta = 0.35\ s^{-1}$, and $f = 2.23$ (Altomare et al., 2001). (B) Predicted S4 movement (dashed line; movement^2 and movement^4 denoted with dotted lines), and onset of ionic currents (continuous line).

opening transition (Altomare et al., 2001). However, a recent study suggested that the opening transition is not voltage dependent in HCN channels (Chen et al., 2007). Therefore, it is not clear what the rate-limiting step is during activation of HCN channels and what causes the relatively low sigmoidicity in HCN channel activation.

In the studies reported here, we used voltage clamp fluorometry (VCF) to simultaneously measure the kinetics of the S4 movement and the ionic currents during voltage activation of sea urchin (spHCN) channels, in order to determine the kinetic relationship between S4 movement and channel opening and to test whether gate opening is rate limiting. In VCF, a fluorophore is attached to an introduced cysteine. The fluorescence from the fluorophore is measured in parallel to the ionic or gating current during voltage steps that activate the channel. VCF has been used earlier to detect conformational changes in voltage-gated ion channels as well as pumps and transporters (Mannuzzu et al., 1996; Cha and Bezanilla, 1997; Li et al., 2000; Meinild et al., 2002; Larsson et al., 2004). We here show that fluorophores attached to centrally located S4 residues report mainly on the gating charge movement that occurs before channel opening. Our results for spHCN channels are not compatible with a fast S4 motion and a rate-limiting channel opening as proposed earlier for mammalian HCN channels (Fig. 1 B; Altomare et al., 2001). Instead, our data and modeling suggest that spHCN channels open after only two S4s have moved and that S4 motion is rate limiting during voltage activation of spHCN channels.

MATERIALS AND METHODS

Expression System

All experiments were performed on the sea urchin spHCN channel (provided by U.B. Kaupp, Forschungszentrum Julich, Julich, Germany) heterologously expressed in *Xenopus* oocytes. Site-directed mutagenesis was performed on spHCN cDNA (in the pGEM-HE expression vector) using the QuikChange system (Stratagene). The DNA was linearized with Nhe1 before RNA synthesis and purification using a T7 mMessage mMachine kit (Ambion). 50 nl cRNA (ranging from 2.5 to 50 ng) was injected into each oocyte, and recordings were made by two-electrode voltage clamp 2–5 d after injection.

Two-Electrode Voltage Clamp

Whole-cell ionic and gating currents were measured with the two-electrode voltage clamp technique using an Axon Geneclamp 500B (Axon Instruments, Inc.). Microelectrodes were pulled using borosilicate glass, filled with a 3 M KCl solution; each microelectrode had a resistance between 0.5 and 1.5 MΩ. All experiments were performed at room temperature. The bath solution contained, in mM: 89 KCl, 10 HEPES, 0.4 $CaCl_2$, and 0.8 $MgCl_2$. The pH was adjusted to 7.4 with KOH, yielding a final K concentration of 100 mM. Data were filtered at 1 kHz, digitized at 5 kHz (Axon Digidata 1322A), and monitored and collected using pClamp software (Axon Instruments, Inc.).

Voltage Clamp Fluorometry

For VCF experiments, oocytes were incubated for 5–30 min (typically 20 min) to saturate binding in a bath solution that was supplemented with 100 μM Alexa-488 C5-Maleimide (Molecular Probes). After washing, oocytes were placed animal pole "up" in a bath housed on a Leica DMLFS upright fluorescence microscope. Light was focused on the animal pole of the oocyte through a 20× objective and was passed through a filter cube from Chroma 41026 (HQ495/30x, Q515LP, HQ545/50m). Fluorescence signals were low-pass Bessell filtered (Frequency Devices) at 200 Hz and digitized at 1 kHz.

Modeling

To create a theoretical framework for understanding the relationship between voltage sensor movement and activation gating in HCN channels, we created several variations on the 10-state model suggested by Altomare et al. (2001). The ionic currents and the S4 movements in Fig. 1 were simulated with an in-house computer program using the 10-state model suggested by Altomare et al. (2001) with the rate constants proposed for the mammalian HCN1 channel (Altomare et al., 2001). For the fits of the different models to the experimental fluorescence and current data in Figs. 6 and 7, we used the fit routine in the Madonna program. For these fits, the gate transition was assumed to be voltage

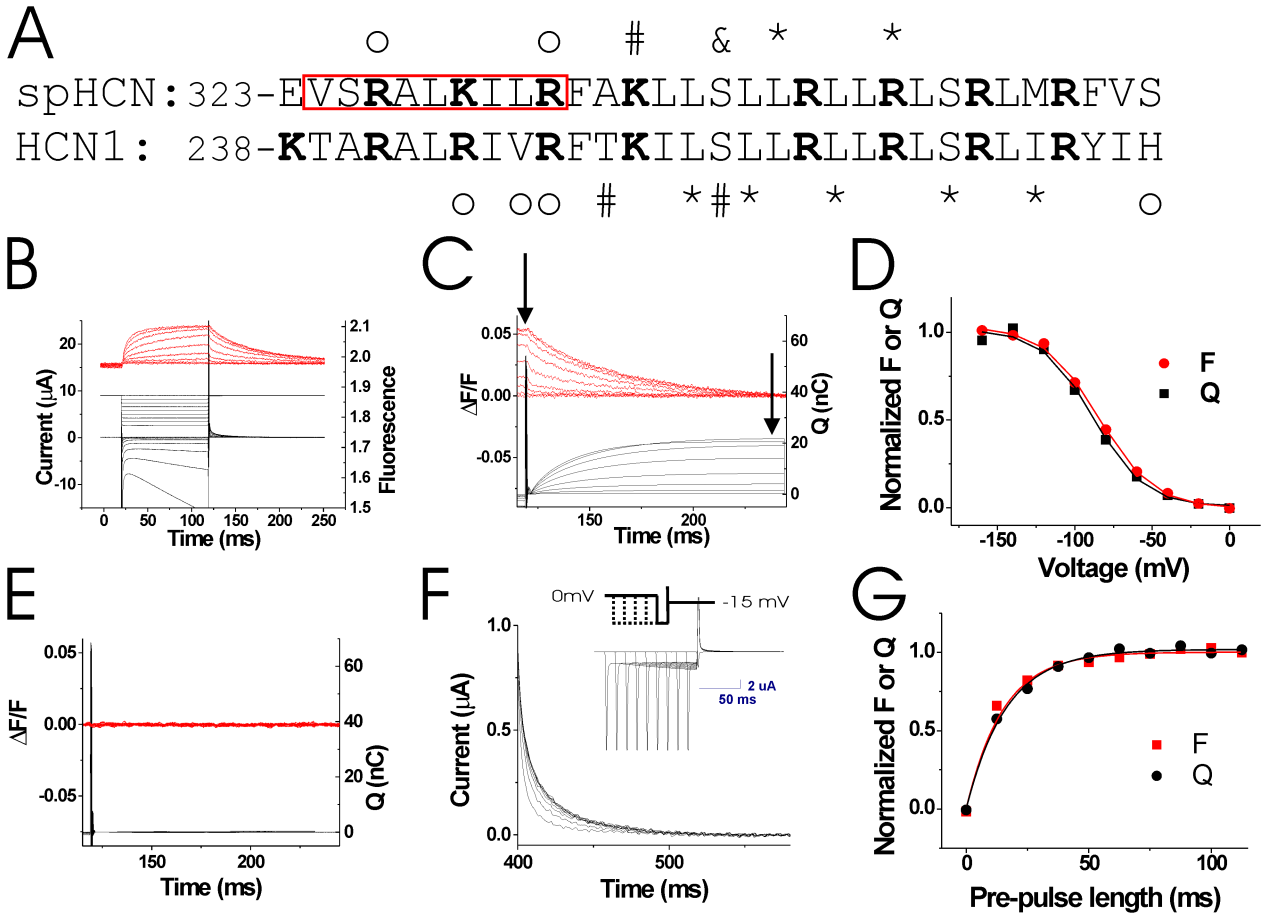

Figure 2. Fluorescence from 332C reports on gating charge movement. (A) Sequence alignment of spHCN and HCN1 S4 domains. The red box highlights residues studied with VCF. Marked residues exhibit state-dependent modification by intracellular (*), extracellular (#), or both intra- and extracellular reagents (&), or state-independent modification by either intracellular or extracellular reagents (o) (Mannikko et al., 2002; Bell et al., 2004; Vemana et al., 2004). (B) Current (bottom, black) and fluorescence (top, red) from Alexa-488–labeled 332C/435Y channels in response to voltage steps from 0 to −160 mV (middle). The P435Y mutation has earlier been shown to render spHCN channels nonconducting (Mannikko et al., 2005). Currents at very negative potentials are from endogenous hyperpolarization-activated chloride channels. (C) Integrated gating charge (bottom, black) from tail currents in B and fluorescence (top, red), showing similar time courses of Q and F. Integration started 1 ms after the voltage pulse to allow complete settling of the capacitive transient. (D) Q(V) and F(V) (measured at arrows in C), showing similar voltage dependence of the gating charge and the fluorescence. Q: $V_{1/2} = -90.7 \pm 8.4$ mV, $z = 1.44 \pm 0.35$; F: $V_{1/2} = -85.3 \pm 9.4$ mV, $z = 1.32 \pm 0.17$ ($P > 0.1$; $n = 7$). (E) Charge movement (bottom, black) and fluorescence (top, red) from uninjected oocytes in response to an identical voltage protocol as in A. (F) Q_{off} gating currents measured at −15 mV in response to longer and longer ($\Delta t = 12.5$ ms) prepulses to −120 mV. Inset shows voltage protocol and currents during the protocol. (G) Integrated gating charge Q_{off} (black) as a function of prepulse length (from F) and normalized fluorescence change (red) measured simultaneously during the prepulse fitted with single exponential curves.

independent, since a recent study suggested that the mammalian HCN1 and HCN2 channels have a voltage-independent gate transition (Chen et al., 2007). This assumption did not qualitatively affect our conclusions, since adding voltage dependence to the closed–open transitions in the 10-state model had little effect on the fit and a negligible effect on the rate of S4 movement relative to the rate of the gate transition.

RESULTS

Fluorescence from Residue 332 Correlates with Gating Charge Movement

To measure conformational changes in S4 during HCN channel activity, we introduced a cysteine at position R332 in the N-terminal region of S4, close to the S4 region that displayed state-dependent accessibility (Fig. 2 A). To directly test whether the fluorescence from 332C channels correlates with the gating charge movement of S4 in spHCN channels, we introduced the P435Y mutation in 332C channels to render the channels nonconducting (Mannikko et al., 2005). We labeled the 332C/435Y channels with the cysteine-specific fluorophore Alexa-488-maleimide and used VCF to monitor gating currents and fluorescence simultaneously under two-electrode voltage clamp (Fig. 2 B). Due to the endogenous currents that are activated in oocytes by the large hyperpolarizing voltage steps needed to activate 332C

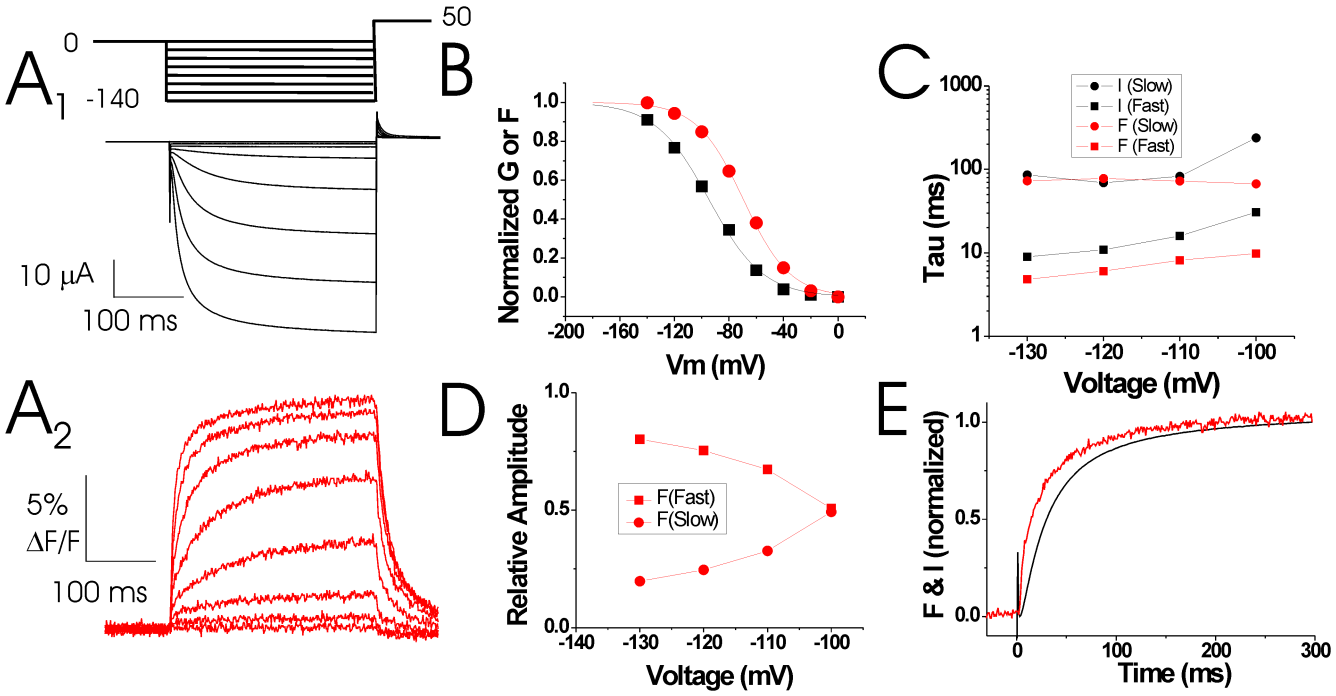

Figure 3. Fluorescence from 332C precedes channel opening. (A) Representative current (A_1) and fluorescence (A_2) records from Alexa-488-maleimide–labeled 332C channels. Channels were held at 0 mV and then stepped to negative potentials (0 to −140 mV, ΔV = 20 mV), followed by a step to +50 mV. (B and C) Steady-state (B) and kinetic analysis (C) of the voltage dependence of the conductance (black symbols) and fluorescence (red symbols) from A. The current and the fluorescence signals were fitted with double exponentials. (D) Amplitudes of the fast (■) and slow (●) fluorescent components from A_2. (E) Normalized currents and fluorescence from A during a step to −120 mV. Note that the fluorescence signal precedes the currents, as expected if S4 movement causes channel opening.

channels, we were unable to accurately and consistently measure the kinetics of the gating currents from 332C channels during the hyperpolarizing steps. However, by measuring the Q_{off} close to the reversal potential for the endogenous chloride currents, estimated around −15 to −10 mV (Weber et al., 1995a,b; Centinaio et al., 1997), we were able to compare the voltage dependence (Fig. 2, C and D) and kinetics (Fig. 2, F and G) of the fluorescence and the gating charge movement. Fig. 2 C shows simultaneous tail fluorescence and Off-gating charge (integrated tail gating currents) recordings. The steady-state values (measured at the arrows) are almost identical (Fig. 2 D). Experiments with 332C channels blocked by 1 mM ZD7288 (a specific HCN-channel blocker) showed similar results (not depicted), while uninjected oocytes did not show any gating currents (Fig. 2 E). To test whether the fluorescence from 332C channels correlates in time with the movement of the gating charge, we measured the development of the Q_{off} after increasingly longer prepulses to −120 mV (Fig. 2 F). Q_{off} and fluorescence developed with similar time courses during the prepulse (τ_Q = 20.8 ± 8.5 ms, τ_F = 19.9 ± 5.6 ms; n = 4), showing that the fluorescence from 332C channels correlates in time with the movement of gating charge (Fig. 2 G). The similar kinetics and voltage dependence of the fluorescence and the gating charge movement strongly suggest that the fluorescence from Alexa-488–labeled 332C channels reports on the gating charge movement of S4 that is hypothesized to precede the ionic current.

Fluorescence from Residue 332 Precedes Channel Opening

To measure both S4 movement and ionic currents in spHCN channels, we introduced the R332C mutation in conducting spHCN channels and used VCF to monitor ionic currents and fluorescence simultaneously under two-electrode voltage clamp. Fig. 3 A shows the ionic currents and fluorescence signals from Alexa-488–labeled 332C channels. The conductance versus voltage, G(V), relationship was shifted by more than −40 mV compared with wt spHCN channels, as reported earlier for 332C channels (Mannikko et al., 2002). Alexa-488–labeled 332C channels showed a left-shifted G(V) relative to the fluorescence versus voltage, F(V), relationship (G: $V_{1/2}$ = −109 ± 11 mV, n = 3; F: $V_{1/2}$ = −79 ± 3 mV; n = 5), so that at small hyperpolarizations (−40 mV) only a fluorescence signal was seen (Fig. 3 B). At hyperpolarizations more negative than −80 mV, both the ionic current and the fluorescence increased with a biexponential time course. The fast component of the fluorescence preceded the ionic current, while the slow component of the fluorescence signal was similar to the slow component of the current (Fig. 3, A and C).

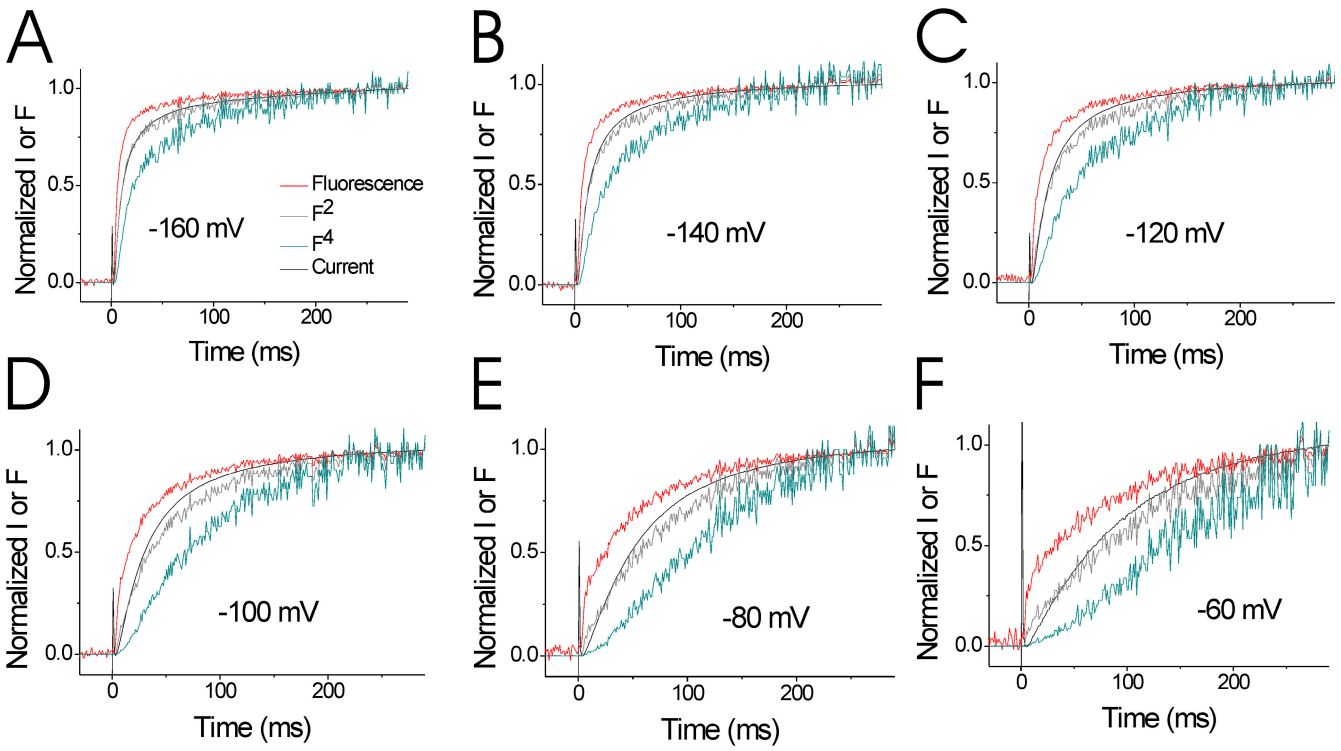

Figure 4. Time course of fluorescence relative to the ionic current. Relative comparison of the fluorescence and the ionic current for steps to indicated voltages. The fluorescence signal is also shown to powers of 2 (F^2) and 4 (F^4). The fluorescence signals to a power of 2 overlap very well with the currents at −160 to −120 mV.

With increasingly larger hyperpolarizations, the amplitude of the slow fluorescence signal decreased and the fluorescence signal became dominated by the fast component (Fig. 3 D), so that the fluorescence signal clearly preceded the current (Fig. 3 E). The voltage and time dependence of the currents and the fluorescence signals from the 332C-labeled channels suggest that 332C-linked fluorophores reported mainly on conformational changes underlying the S4 gating charge movement that precedes channel opening.

Fluorescence Signal Raised to a Power of Two Correlates with the Current

To gain insight into the kinetic relationship between S4 movement and activation gating, we compared the time course of the fluorescence from 332C-labeled channels to the time course of the ionic current from the same channels in response to different voltage steps.

In Fig. 4, we show the normalized fluorescence change and ionic current for voltage steps between −60 and −160 mV. We also show the fluorescence signal raised to different powers. We then compare these data to the predictions of the relationship between S4 motion and the ionic current for the model shown in Fig. 1. For voltage steps to −120 mV and more negative, the normalized fluorescence signal raised to a power of two superimposed well on the normalized current trace (Fig. 4, A–C), suggesting that only two independent events preceded channel opening (see Discussion). At less negative voltage steps, the current deviated from fluorescence signal to a power of two (Fig. 4, D and E). At these voltages, the current and the fluorescence had a similar time course after the initial delay in the ionic current and the initial small, fast component of the fluorescence. The kinetic relationship between S4 motion and the onset of the ionic current at all voltages is very different from the one predicted by the model in Fig. 1 B, which suggests that spHCN channels do not have a fast S4 movement and a rate-limiting gate transition.

Outer S4 Residues Report on Two Distinct Conformational Changes

To measure conformational changes at more residues in S4 during HCN channel activity, we introduced a cysteine at nine contiguous positions in the N-terminal region of S4 (red box in Fig. 2 A). We labeled the cysteines with the cysteine-specific fluorophore Alexa-488-maleimide and used VCF to monitor current and fluorescence simultaneously under two-electrode voltage clamp. Eight of nine residues provided fluorescence signals when labeled with Alexa-488-maleimide. Residue 329C had very small ionic currents and did not give a fluorescence signal. Fluorescence changes from residues 324C-326C were shown in a recent paper to report on the mode shift in HCN channel voltage dependence (Bruening-Wright and Larsson, 2007).

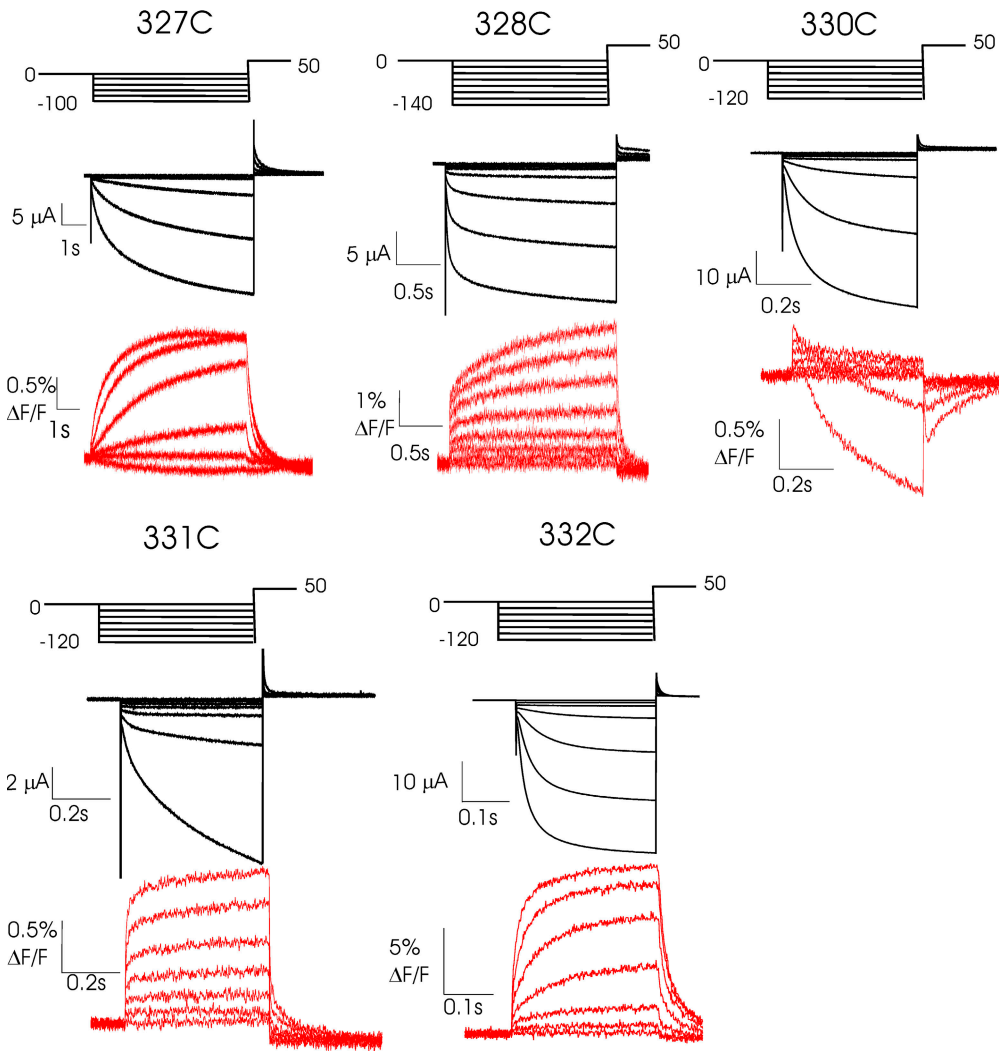

Figure 5. Fluorescence from N-terminal S4 residues. Representative current (top, black) and fluorescence (bottom, red) records for Alexa-488-maleimide–labeled residues 327C–332C. Channels were held at 0 mV and then stepped to negative potentials (0 to −140 mV, ΔV = 20 mV), followed by a step to +50 mV. Note that residues (328–332C) all have fast fluorescence signals that preceded channel opening, presumably because they report on S4 movement during the gating charge translocation.

In Fig. 5, ionic currents and fluorescence signals are shown for the remaining five S4 residues that provided a fluorescence signal. Residues 327C–332C all had large fluorescent components that were faster than the kinetics of channel opening (Table I). In addition, two of these residues (328C and 330C) had a second fluorescent component that changed more slowly than channel activation and most likely tracked the mode shift described by Männikkö et al. (Bruening-Wright and Larsson, 2007). The two fluorescent components from the 330C channels had opposite polarity, which shows that the fluorophore reports on two distinct conformational changes in/around S4. We did not further analyze the fluorescence and the ionic current from residues 327C–331C, since these channels had very slow activation kinetics (e.g., 327C and 331C) or additional fluorescence component that complicated the analysis (e.g., 330C). However, residues 327C–331C all had large fluorescent components that were faster than the kinetics of channel opening, similar to 332C channels, suggesting that these sites track the S4 transmembrane movement that precedes channel opening (Table I). In contrast, we have previously shown that residues 324–326 all have only slow fluorescence changes, slower than channel activation (Bruening-Wright and Larsson, 2007). The fluorescence from these external residues correlated with the mode shift in HCN channel voltage dependence, suggesting that these residues only track the slower mode shift.

10-State Model Can Reproduce the Kinetic Relationship between the S4 Movement and Gate Opening

We next simultaneously fitted the fluorescence and the ionic currents from 332C channels to a 10-state allosteric model similar to the model by Altomare et al. (Fig. 1 A). A recent study suggested that the opening transition in mammalian HCN channels is not voltage dependent (Chen et al., 2007). We therefore assumed nonvoltage-dependent transitions between the closed and open states, while using voltage-dependent transitions between closed states and between open states. The assumption of nonvoltage-dependent opening transitions did not

TABLE I

Time Constants (τ) and Amplitudes (A) for Current (I) and Fluorescence (F) from Experiments Similar to Fig. 5

Residue	τ_{1I}	τ_{2I}	$A_1/(A_1+A_2)_I$	τ_{1F}	τ_{2F}	$A_1/(A_1+A_2)_F$	*n*
327C	1238 ± 190	N/A	N/A	884 ± 157	N/A	N/A	4
328C	38 ± 5	334 ± 22	0.59 ± 0.07	9.5 ± 1.5	631 ± 109	0.49 ± 0.04	3
329C	N/A	N/A	N/A	N/A	N/A	N/A	
330C	152 ± 32	2696 ± 476	0.46 ± 0.05	5.7 ± 2.1	4919 ± 1091	0.06 ± 0.02	3
331C	24 ± 1	396 ± 42	0.19 ± 0.04	4.5 ± 0.2	122 ± 7	0.77 ± 0.02	4
332C	18 ± 5	135 ± 31	0.46 ± 0.09	5.9 ± 0.8	62 ± 5	0.27 ± 0.02	5

Voltage step to −120 mV. τ in ms. For residue 327, I and F were well fit with a single exponential at −120 mV. For residues 328–332, two exponentials were needed to get good fits. 329C did not express well enough to give a clear fluorescence signal.

qualitatively influence the outcome of the modeling (see below). Fig. 6 A shows the best fit of the 10-state model to the ionic and fluorescence data from Alexa-488–labeled R332C channels. We did not fit the fluorescence and ionic currents during the tail potentials, because the tail kinetics are dominated by the mode shift (which is not represented in the 10-state model) (Mannikko et al., 2005) and because the size of the outward tail currents is not proportional to the inward currents during the hyperpolarizing steps due to the presence of an endogenous voltage-dependent blocker of HCN channels in oocytes (Vemana, S., personal communication; unpublished data). The kinetics of the fluorescence and the ionic currents are fairly well reproduced, although not perfectly, by the 10-state model. The 10-state model did, however, generate a kinetic relationship between the fluorescence and the ionic currents that was very similar to the kinetic relationship between the fluorescence and the ionic current for 332C channels, i.e., the fluorescence raised to a power of two superimposed well on the ionic currents (Fig. 6, B and C). The fitted rates for the S4 movement (α) were slower than the closed-to-open transition for the state with all S4s activated (γ). This is in contrast to the kinetic relationship of α and γ predicted by the model suggested previously for mammalian HCN channels (Fig. 1 A), which had a rate-limiting channel opening and a fast S4 movement to generate the low sigmoidicity in the ionic currents (Fig. 1 B; Altomare et al., 2001). In our model, the low sigmoidicity in spHCN channels is caused by channel opening after only two S4s have moved and a non rate-limiting opening transition. If voltage dependence is included in the opening transition in the 10-state model, as it is in the model by Altomare et al., the fit of the data is not greatly improved (χ^2 = 15.9 versus 16.6), and our main conclusion that the opening transition is not rate limiting still holds true (unpublished data).

Addition of Two Different Types of Cooperativity in S4 Motion Did Not Improve the Fits

The data and modeling we present in this paper suggest that the power-of-two relationship between the S4 movement and ionic currents in spHCN channels can be explained by the spHCN channels opening after only two of the four S4s have moved (Fig. 7 A). A power-of-two relationship can in general also be reproduced by other models in which individual S4 subunits move in a cooperative fashion (for example Fig. 7, B and C). Earlier data (Ulens and Siegelbaum, 2003) are consistent with the idea of cooperativity among subunits during HCN channel activation. Based on biophysical analysis of cAMP binding site mutant channels, it was suggested that the C termini (the ligand-binding domains) of HCN channels function as a dimer-of-dimers, in which each of the two dimers act independently. However, the recent crystal structure of the C termini of HCN2 was shown to be a fourfold symmetrical structure, not a dimer-of-dimers structure (Zagotta et al., 2003). One possibility to explain this apparent discrepancy is that the asymmetry is not in the ligand-binding domain, but that the asymmetry is really in the transmembrane portions of the subunits. A dimer-of-dimers organization of the transmembrane domains could generate the same type of "asymmetric" data from linked channels (Ulens and Siegelbaum, 2003). If the two S4s in the two subunits that form each dimer move in a cooperative fashion, then this dimer-of-dimers model for HCN channel activation could also potentially display a power-of-two relationship between the S4 fluorescence and the ionic current. Another type of cooperativity model that has been proposed for voltage-activated ion channels is a model in which each activated S4 equally influences the other S4s by a constant factor (Zagotta et al., 1994a). This type of cooperativity could also potentially generate a power-of-two relationship between the S4 fluorescence and the ionic current. We therefore fit two different "cooperativity models" (variants of the 10-state model) to our data (Fig. 7, B and C) to test whether these types of cooperativity in S4 movement would improve the fits. The first model had cooperativity among all S4s, where each activated S4 increased the rate of activation of the other S4s by a constant cooperativity factor (Fig. 7 B). This model did not give a better fit to our data, since the best fit of this model yielded a cooperativity factor of 1. A cooperativity factor of 1 basically

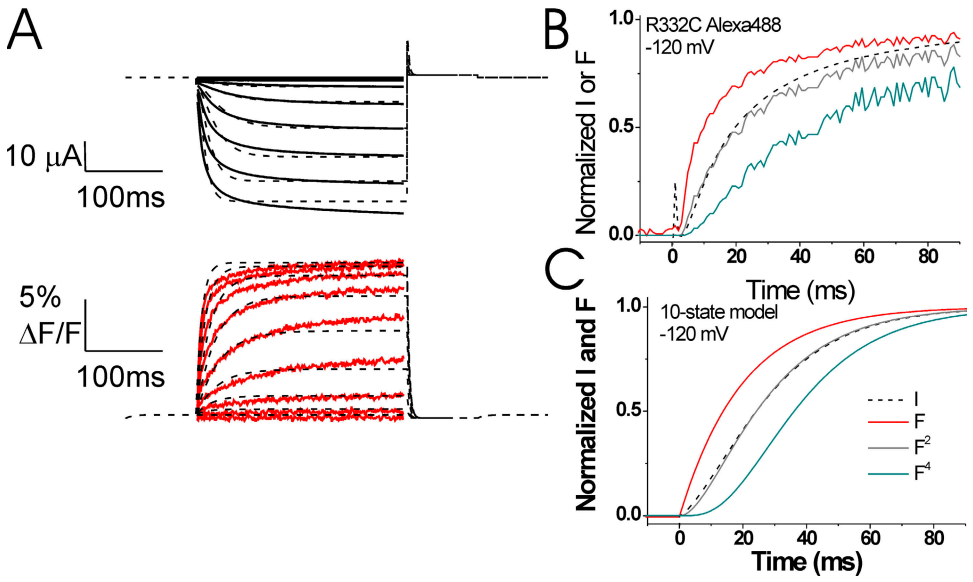

Figure 6. A modified 10-state model reproduces the experimental data. (A) Representative current (black lines) and fluorescence (red lines) records from Alexa-488-maleimide–labeled 332C channels (from Fig. 3 A), overlaid with the best fit ($\chi^2 = 16.6$) from our 10-state model (dashed line; see parameter values in Table II). In this model, the fluorescence changes only during the rate-limiting S4 gating charge movement (see Fig. 8). (B and C) Normalized currents and fluorescence from B Alexa-488–labeled 332C channels (data from Fig. 4 C) and (C) the 10-state model during a step to −120 mV. Note that the fluorescence signal precedes the currents, as expected if S4 movement causes channel opening. The fluorescence to a power of 2 (F^2) and to a power of 4 (F^4) is also shown for each case. The currents are similar to the F^2 curve for both the experimental data and for the 10-state model, whereas the F^4 curve follows after the current in the both the experimental data and the 10-state model.

means that the model reverted to the earlier 10-state model without cooperativity (Fig. 7 A). A second cooperative model we used was the dimer-of-dimers model described above (Fig. 7 C). The fit of the dimer-of-dimers model did not give a significantly better quantitative fit to our data (Fig. 7 D; $\chi^2 = 16.9$ versus 16.6 for the 10-state model). In the dimer-of-dimers model, the ionic currents clearly preceded the fluorescence to a power of two (Fig. 7 E). Compared with the 10-state model, the fitted dimer-of-dimers model did less well in reproducing the finding that the fluorescence signal to a power of two overlapped with the ionic currents at hyperpolarized potentials (compare Fig. 7 E with Fig. 6). Therefore, we conclude that incorporating these two types of cooperative gating in HCN channels did not improve the fits to our data compared with our original 10-state model. Nonetheless, other types of cooperativity in HCN channels could easily be envisioned, and we cannot rule out "cooperativity models" in general based on the data and modeling presented here.

DISCUSSION

Fluorescence signals and currents from fluorophore-labeled cysteine mutants suggest two distinct movements of S4 in HCN channels: a fast conformational change that carries gating charge and precedes channel opening and a slower conformational change during the mode shift that follows channel opening (see Bruening-Wright and Larsson, 2007). We found that the conformational changes during gating-charge movement were reported by residues C terminal to residue 326, while the conformational changes during the mode shift extended to more N terminally located S4 residues (324C, 325C, and 326C). That these more external S4 residues do not report on the gating charge movement whereas the more C-terminal residues do report on the gating charge movement is consistent with earlier accessibility studies (Fig. 2 A; Mannikko et al., 2002; Bell et al., 2004; Vemana et al., 2004).

Proposed Model for HCN Channel Activation

Taking into consideration both the fluorescence and the cysteine accessibility data, we propose the following model of HCN channel activation by hyperpolarization (Fig. 8). (1) In response to the hyperpolarization, the S4 helix moves inward (i.e., a gating charge movement), burying external residues up to residue 332. The more

TABLE II

Fitted Parameters for Models in Figs. 6 and 7

	10-State	Cooperativity	Dimer-of-dimers
χ^2	16.6	17.0	16.9
K_{ab} [ms^{-1}]	0.0157	0.016	0.0076
Z_{ab} [e_0]	0.60	0.60	0.625
V_{ab} [mV]	−78.2	−78.4	−78.4
c	N/A	1.0	N/A
γ [ms^{-1}]	0.40	0.29	0.27
δ [ms^{-1}]	0.40	0.32	1.0
f	1.57	1.55	1.53

The only voltage-dependent transitions in the models are the rates determining the S4 movement: $\alpha = K_{ab} \exp(-Z_{ab}(V - V_{ab})/kT)$ and $\beta = K_{ab} \exp(+Z_{ab}(V - V_{ab})/kT)$. The other rates are all voltage independent.

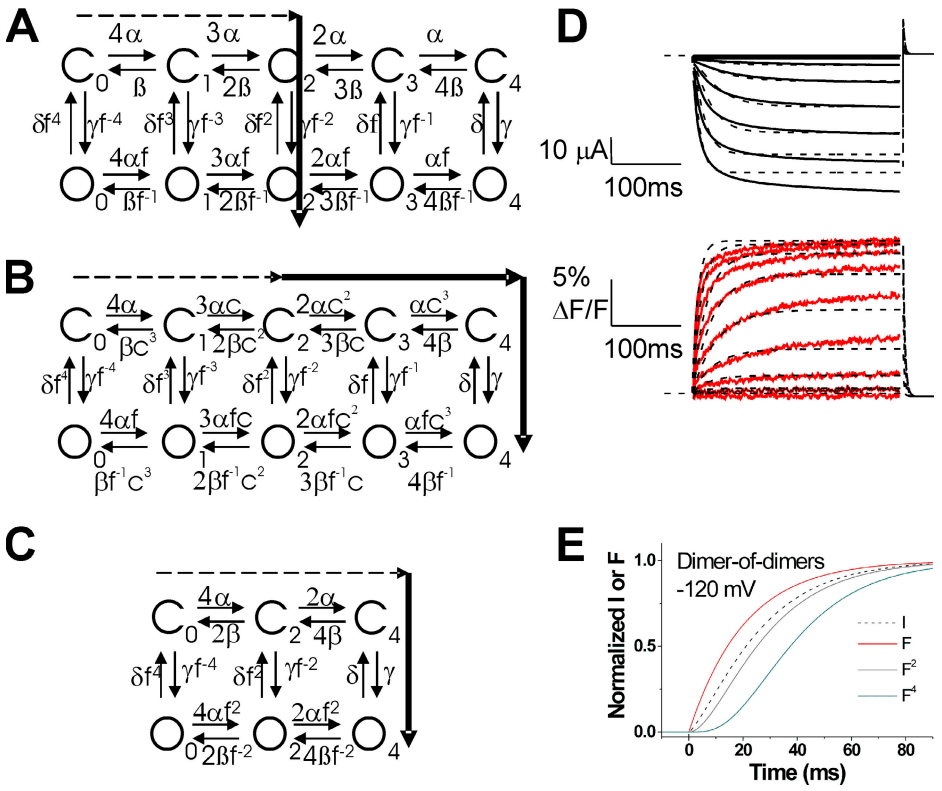

Figure 7. Cooperative models did not improve the fits. (A–C) Different possible models for HCN channel opening generating $F^2 = I$ relationship. The arrows through the state diagrams denote the most likely transition pathway. Continuous arrows denote fast transitions and dashed lines slow transitions. (A) An allosteric model with four independent S4 movements with a non rate-limiting activation-gate transition. This is the model used in Fig. 6. (B) An allosteric model with cooperative S4 movements, in which the movement of each S4 affects the movement of the other S4s by a constant factor c. A similar model was suggested for negative cooperativity in S4 movement in Shaker K channels (Zagotta et al., 1994a). (C) A dimer-of-dimers model for S4 activation of HCN channels as earlier proposed (DiFrancesco, 1999; Ulens and Siegelbaum, 2003). (D) Representative current (black lines) and fluorescence (red lines) records from Alexa-488-maleimide–labeled 332C channels (from Fig. 3 A), overlaid with the best fit ($\chi^2 = 16.9$) from the dimer-of-dimers model (dashed lines; see parameter values in Table II). In this model, the fluorescence changes only during the rate-limiting S4 gating charge movement. (E) Normalized currents and fluorescence from the dimer-of-dimers model from D during a step to −120 mV. The fluorescence to a power of 2 (F^2) and to a power of 4 (F^4) is also shown. The currents clearly precede the F^2 curve in the dimer-of-dimers model. In contrast, the current overlays the F^2 curve in both the experimental data and the 10-state model (Fig. 6, B and C).

N-terminal end of S4 remains extracellular. Residues close to 332 report on the transmembrane movement of S4, while residues 324–326, which are further away from this region, do not detect the S4 charge movement, because the S4 movement does not change their accessibility or fluorescence. (2) The transmembrane movement of S4 triggers channel opening. There is no fluorescence change directly due to channel opening. (3) The channel is depolarized, S4 moves up, and fluorescence returns to its baseline value. (4) The channels close. There is no fluorescence change directly due to channel closing.

Comparison of Gating Models

Fluorescence data from 332C suggest that the activation mechanism of spHCN channels may differ both from a traditional Hodgkin-Huxley–type model and from a previously published model for HCN activation (Altomare et al., 2001). As expected for any model in which S4 movement causes channel opening, the fluorescence signal from Alexa-488–labeled 332C channels preceded activation of the current (Fig. 3 E). The prediction for a Hodgkin-Huxley–type model of channel activation, in which a tetrameric channel with four independent S4s opens only after all four S4s have activated, is that the fluorescence signal to a power of four should superimpose on the current. This is not the case for 332C channels. For 332C channels, the fluorescence signal to a power of two superimposed on the current trace (Fig. 4), suggesting that only two independent events precede channel opening and that S4 movement is the rate-limiting step during channel activation in spHCN channels. This kinetic relationship between S4 movement and the onset of the ionic currents is different from that predicted by a previous model for mammalian HCN channels (Altomare et al., 2001), which assumed that the gate opening is the rate-limiting step during channel opening in mammalian HCN channels.

Our model is consistent with a recent study that suggested that the activation rate is voltage independent in mammalian HCN channels at extreme hyperpolarizations (Chen et al., 2007). The data from the Chen et al. study suggests that the closed-to-open transition is voltage independent in mammalian HCN channels and that this transition becomes rate limiting at extreme hyperpolarizations (e.g., more negative than −140 mV for HCN2 channels). However, at physiological hyperpolarizations (more positive than −100 mV), the mammalian HCN channels display a steep voltage dependence in the opening rate. Therefore, even in mammalian

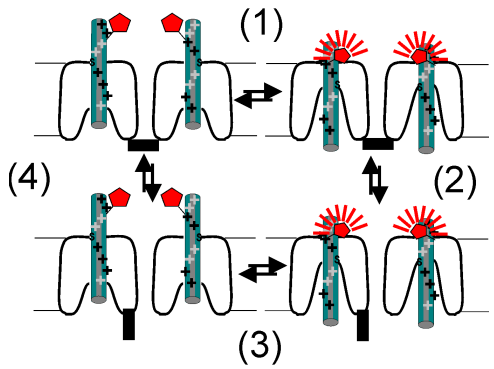

Figure 8. Model for fluorescence from S4 during HCN channel gating. Proposed model for how the S4 movement in HCN channels generates the fluorescence data from 332C channels. The S4 movement (1) in the different subunits is assumed to be independent. The proposed model for the transmembrane movement of S4 charges, with both a vertical S4 movement and a simultaneous opening of an intracellular crevice, is a combination of two models earlier proposed for HCN channels (Mannikko et al., 2002; Bell et al., 2004; Vemana et al., 2004). Channel opening (2) is assumed to be by concerted, allosteric conformational changes in all four subunits. For simplicity, only two, out of the four, subunits are shown. S4 is shown in green, the intracellular activation gate is black, and the fluorophore is shown in red (more fluorescence intensity is shown with more and thicker radiating lines). Fluorescence from the gating charge-carrying region of the voltage sensor (i.e., from 332C), increases when the gating charge-carrying portion of S4 moves down in response to hyperpolarization (1), but does not change during as a direct result of channel opening (2). Fluorescence decreases when S4 moves up in response to depolarization (3), but does not change as a direct result of channel closing (4).

HCN channels, it is likely that at physiological voltages the S4 movement is the rate-limiting step during activation and that the closed-to-open transition is not rate limiting. We have not been able to measure any gating currents from the mammalian HCN channels to directly test the kinetic relationship between S4 movement and the gate opening in mammalian HCN channels (unpublished data). The reason for this is not clear, but could be due to slower S4 movement and lower expression levels of mammalian HCN channels compared with spHCN channels.

The data and modeling we present in this paper suggest that the power-of-two relationship between the S4 movement and ionic currents in spHCN channels can be explained if the spHCN channels open after only two of the four S4s have moved (Fig. 7 A). We also concluded that incorporating two different types of cooperative gating in HCN channels did not improve the fits to our data compared with our original 10-state model (Fig. 7). Nonetheless, other types of cooperativity in HCN channels could easily be envisioned, and we cannot rule out "cooperativity models" in general based on the data and modeling presented here. Further experiments using linked tetrameric channels composed of subunits with different midpoints of activation (Mannuzzu and Isacoff, 2000; Ulens and Siegelbaum, 2003) are needed to determine whether the movement of two S4s is sufficient to gate HCN channels or if there is some type of cooperativity in the activation of S4s in HCN channels.

In summary, our data suggest that during activation gating in HCN channels the movement of S4 is rate limiting, not gate opening, and that the channels may open before all S4s have activated. This mechanism is distinct from models used for other voltage-gated channels, e.g., most models suggest that Shaker K channels open only after all four S4s have activated (Zagotta et al., 1994a,b; Schoppa and Sigworth, 1998a,b,c). The mechanism we present is also different from the prediction of the most common model of HCN channel gating (Altomare et al., 2001). Finally, our data suggest that S4 in HCN channels undergoes at least two kinetically distinct movements during gating. It will be interesting to determine in future experiments the molecular mechanism by which these voltage sensor movements are coupled to the activation gate.

We thank James Maylie, Jeff Karpen, and John Adelman for helpful comments on the manuscript, and Sandra Oster for editing the manuscript.

This work was supported by American Heart Association grant 0425914Z (A. Bruening-Wright), the Swedish Research Council no. 13043 (F. Elinder), the Swedish Heart-Lung Foundation (F. Elinder), and National Institutes of Health grant NS043259 (H.P. Larsson).

Olaf S. Andersen served as editor.

Submitted: 28 February 2007
Accepted: 1 June 2007

REFERENCES

Altomare, C., A. Bucchi, E. Camatini, M. Baruscotti, C. Viscomi, A. Moroni, and D. DiFrancesco. 2001. Integrated allosteric model of voltage gating of HCN channels. *J. Gen. Physiol.* 117:519–532.

Bell, D.C., H. Yao, R.C. Saenger, J.H. Riley, and S.A. Siegelbaum. 2004. Changes in local S4 environment provide a voltage-sensing mechanism for mammalian hyperpolarization-activated HCN channels. *J. Gen. Physiol.* 123:5–19.

Brown, H., and D. DiFrancesco. 1980. Voltage-clamp investigations of membrane currents underlying pace-maker activity in rabbit sino-atrial node. *J. Physiol.* 308:331–351.

Bruening-Wright, A., and H.P. Larsson. 2007. Slow conformational changes of the voltage sensor during the mode shift in hyperpolarization-activated cyclic-nucleotide-gated channels. *J. Neurosci.* 27:270–278.

Centinaio, E., E. Bossi, and A. Peres. 1997. Properties of the Ca^{2+}-activated Cl^- current of *Xenopus* oocytes. *Cell. Mol. Life Sci.* 53:604–610.

Cha, A., and F. Bezanilla. 1997. Characterizing voltage-dependent conformational changes in the Shaker K^+ channel with fluorescence. *Neuron.* 19:1127–1140.

Chen, S., J. Wang, L. Zhou, M.S. George, and S.A. Siegelbaum. 2007. Voltage sensor movement and cAMP binding allosterically regulate an inherently voltage-independent closed-open transition in HCN channels. *J. Gen. Physiol.* 129:175–188.

DiFrancesco, D. 1984. Characterization of the pace-maker current kinetics in calf Purkinje fibres. *J. Physiol.* 348:341–367.

DiFrancesco, D. 1993. Pacemaker mechanisms in cardiac tissue. *Annu. Rev. Physiol.* 55:455–472.

DiFrancesco, D. 1999. Dual allosteric modulation of pacemaker (f) channels by cAMP and voltage in rabbit SA node. *J. Physiol.* 515:367–376.

Gauss, R., R. Seifert, and U.B. Kaupp. 1998. Molecular identification of a hyperpolarization-activated channel in sea urchin sperm. *Nature.* 393:583–587.

Hille, B. 2001. Ion Channels of Excitable Membranes. Third Edition. Sinauer Associates, Inc., Sunderland, MA. 814 pp.

Larsson, H.P., A.V. Tzingounis, H.P. Koch, and M.P. Kavanaugh. 2004. Fluorometric measurements of conformational changes in glutamate transporters. *Proc. Natl. Acad. Sci. USA.* 101:3951–3956.

Li, M., R.A. Farley, and H.A. Lester. 2000. An intermediate state of the γ-aminobutyric acid transporter GAT1 revealed by simultaneous voltage clamp and fluorescence. *J. Gen. Physiol.* 115:491–508.

Ludwig, A., T. Budde, J. Stieber, S. Moosmang, C. Wahl, K. Holthoff, A. Langebartels, C. Wotjak, T. Munsch, X. Zong, et al. 2003. Absence epilepsy and sinus dysrhythmia in mice lacking the pacemaker channel HCN2. *EMBO J.* 22:216–224.

Mannikko, R., F. Elinder, and H.P. Larsson. 2002. Voltage-sensing mechanism is conserved among ion channels gated by opposite voltages. *Nature.* 419:837–841.

Mannikko, R., S. Pandey, H.P. Larsson, and F. Elinder. 2005. Hysteresis in the voltage dependence of HCN channels: conversion between two modes affects pacemaker properties. *J. Gen. Physiol.* 125:305–326.

Mannuzzu, L.M., and E.Y. Isacoff. 2000. Independence and cooperativity in rearrangements of a potassium channel voltage sensor revealed by single subunit fluorescence. *J. Gen. Physiol.* 115:257–268.

Mannuzzu, L.M., M.M. Moronne, and E.Y. Isacoff. 1996. Direct physical measure of conformational rearrangement underlying potassium channel gating. *Science.* 271:213–216.

Maylie, J., and M. Morad. 1984. Ionic currents responsible for the generation of pace-maker current in the rabbit sino-atrial node. *J. Physiol.* 355:215–235.

Maylie, J., M. Morad, and J. Weiss. 1981. A study of pace-maker potential in rabbit sino-atrial node: measurement of potassium activity under voltage-clamp conditions. *J. Physiol.* 311:161–178.

Meinild, A.K., B.A. Hirayama, E.M. Wright, and D.D. Loo. 2002. Fluorescence studies of ligand-induced conformational changes of the Na^+/glucose cotransporter. *Biochemistry.* 41:1250–1258.

Nolan, M.F., G. Malleret, K.H. Lee, E. Gibbs, J.T. Dudman, B. Santoro, D. Yin, R.F. Thompson, S.A. Siegelbaum, E.R. Kandel, and A. Morozov. 2003. The hyperpolarization-activated HCN1 channel is important for motor learning and neuronal integration by cerebellar Purkinje cells. *Cell.* 115:551–564.

Pape, H.C. 1996. Queer current and pacemaker: the hyperpolarization-activated cation current in neurons. *Annu. Rev. Physiol.* 58:299–327.

Schoppa, N.E., and F.J. Sigworth. 1998a. Activation of shaker potassium channels. I. Characterization of voltage-dependent transitions. *J. Gen. Physiol.* 111:271–294.

Schoppa, N.E., and F.J. Sigworth. 1998b. Activation of Shaker potassium channels. II. Kinetics of the V2 mutant channel. *J. Gen. Physiol.* 111:295–311.

Schoppa, N.E., and F.J. Sigworth. 1998c. Activation of Shaker potassium channels. III. An activation gating model for wild-type and V2 mutant channels. *J. Gen. Physiol.* 111:313–342.

Schulze-Bahr, E., A. Neu, P. Friederich, U.B. Kaupp, G. Breithardt, O. Pongs, and D. Isbrandt. 2003. Pacemaker channel dysfunction in a patient with sinus node disease. *J. Clin. Invest.* 111:1537–1545.

Sesti, F., S. Rajan, R. Gonzalez-Colaso, N. Nikolaeva, and S.A. Goldstein. 2003. Hyperpolarization moves S4 sensors inward to open MVP, a methanococcal voltage-gated potassium channel. *Nat. Neurosci.* 6:353–361.

Ueda, K., K. Nakamura, T. Hayashi, N. Inagaki, M. Takahashi, T. Arimura, H. Morita, Y. Higashiuesato, Y. Hirano, M. Yasunami, et al. 2004. Functional characterization of a trafficking-defective HCN4 mutation, D553N, associated with cardiac arrhythmia. *J. Biol. Chem.* 279:27194–27198.

Ulens, C., and S.A. Siegelbaum. 2003. Regulation of hyperpolarization-activated HCN channels by cAMP through a gating switch in binding domain symmetry. *Neuron.* 40:959–970.

Vemana, S., S. Pandey, and H.P. Larsson. 2004. S4 movement in a mammalian HCN channel. *J. Gen. Physiol.* 123:21–32.

Weber, W.M., K.M. Liebold, F.W. Reifarth, and W. Clauss. 1995a. The Ca^{2+}-induced leak current in *Xenopus* oocytes is indeed mediated through a Cl^- channel. *J. Membr. Biol.* 148:263–275.

Weber, W.M., K.M. Liebold, F.W. Reifarth, U. Uhr, and W. Clauss. 1995b. Influence of extracellular Ca^{2+} on endogenous Cl^- channels in *Xenopus* oocytes. *Pflugers Arch.* 429:820–824.

Zagotta, W.N., T. Hoshi, and R.W. Aldrich. 1994a. Shaker potassium channel gating. III: Evaluation of kinetic models for activation. *J. Gen. Physiol.* 103:321–362.

Zagotta, W.N., T. Hoshi, J. Dittman, and R.W. Aldrich. 1994b. Shaker potassium channel gating. II: Transitions in the activation pathway. *J. Gen. Physiol.* 103:279–319.

Zagotta, W.N., N.B. Olivier, K.D. Black, E.C. Young, R. Olson, and E. Gouaux. 2003. Structural basis for modulation and agonist specificity of HCN pacemaker channels. *Nature.* 425:200–205.